Journal of the Serbian Chemical Society
JSCS-info@shd.org.rs • www.shd.org.rs/JSCS
J. Serb. Chem. Soc. *88* (10) 1025–1037 (2023)
JSCS–5678
Original scientific paper
Published 24 October 2023

Impedance response of aluminum alloys with varying Mg content in Al–Mg systems during exposure to chloride corrosion environment

JELENA ŠĆEPANOVIĆ[1], MARIJANA R. PANTOVIĆ PAVLOVIĆ[2,3#], DARKO VUKSANOVIĆ[1], GAVRILO M. ŠEKULARAC[2] and MIROSLAV M. PAVLOVIĆ[2,3#*]

[1]*Faculty of Metallurgy and Technology, University of Montenegro, Podgorica, Montenegro.* [2]*Institute of Chemistry, Technology and Metallurgy, National Institute of the Republic of Serbia, Department of Electrochemistry, University of Belgrade, Belgrade, Serbia and* [3]*Center of Excellence in Environmental Chemistry and Engineering, Institute of Chemistry, Technology and Metallurgy, Belgrade, Serbia*

(Received 5 May, revised 23 June, accepted 1 July 2023)

Abstract: This research discusses the corrosion behavior of as-cast Al alloys with different Mg content by potentiostatic electrochemical impedance spectroscopy (PEIS). The complex plane spectra of all samples feature a high-frequency loop, followed by semi-infinite diffusion impedance characteristics at low frequencies, with the corrosion-induced formation of a defined porous structure of a layer making finite diffusion through the pores dominant upon prolonged exposure. The most compact layer causes the most pronounced and well-resolved finite diffusion features in the impedance spectra of the sample with the highest Mg content, while the sample with the lowest Mg content has a highly porous layer unable to slow down the corrosion rate at the layer/ /sample interface. The highest layer capacitance and diffusion admittance are found in the sample with the highest Mg content, with a more adherent protective film expected to form. However, the growth rate of the layer was not adequate for the remarkable closing of the pits, indicating the weakness of this sample towards pit activity. The results show that increasing Mg content improves corrosion resistance and clearly separates bulky corrosion from localized pitting corrosion, but it also increases the thickness of a more compact, poorly adhesive layer.

Keywords: electrochemical impedance spectroscopy; aluminum alloys; corrosion behavior; chemical composition; mechanical properties.

* Corresponding author. E-mail: miroslav.pavlovic@ihtm.bg.ac.rs
# Serbian Chemical Society member.
https://doi.org/10.2298/JSC230505031S

INTRODUCTION

Aluminum and its alloys have a wide range of applications in industry as well as consumption due to their unique properties, such as light weight, high strength and good corrosion resistance.[1–3] Due to the broad application and economic importance of aluminum and its alloys, increasing attention is being paid to researching the corrosion characteristics of these materials in cast, aged, and technically processed states.[1,4,5] Aluminum–magnesium alloys have been the subject of numerous studies on corrosion rates in various solutions.[5–9] The formation of a protective oxide layer is the main reason behind its excellent corrosion resistance. However, under saline conditions, such as those encountered in marine environments, aluminum alloys are vulnerable to localized degradation in the form of pitting and crevice corrosion. This type of corrosion occurs due to the adsorption of anions, particularly chlorides, at the oxide–solution interface.[5] From the standpoint of corrosion rate, in a chloride environment, Al–Mg alloys are susceptible to localized degradation in the form of pitting corrosion. The highest corrosion rate is observed in alloys containing around 0.8 mass % of magnesium.[4] A higher magnesium content in Al alloys generally indicates a higher degree of surface oxidation, where magnesium content varies from 6 to 8 %.[9,10] The passive stable surface film serves as a barrier for the transfer of cations from the metal to the environment and for the counter diffusion of oxygen and other anions.[11] Chemically homogeneous, single-phase amorphous alloys free from crystalline defects such as precipitates, segregates, grain boundaries and dislocations often create a conducive environment for the formation of a uniform passive film without any weak points.[6] Dragos *et al.*[12] shows results of elongation and structural analysis of Al–Mg alloy before and after heat treatment and artificial aging. On the other hand, alloys with magnesium are structural metals that are lightweight. The lightweight nature of such materials is the main reason for the interest in Al–Mg alloys in various industrial applications.[13]

Aluminum forms a protective oxide film in the pH range 4.0–8.5, but this depends on temperature, form of oxide present and the presence of substances that form soluble complexes or insoluble salts with aluminum. This implies that the oxide film is soluble at pH values below 4.0 and above 8.5. Several investigations reported that the pitting potential of aluminum in chloride solutions is independent of pH in the range 4–9.[14–16] However, pitting corrosion rate was found increased at slightly acidic and alkaline solutions with respect to neutral solutions.

The corrosion behavior of aluminum alloys is significantly affected by the presence of particles in the matrix.[3] Literature data[2,8,14,16,19] showed that Mg_2Si particles tend to be anodic in relation to the matrix and can act as initiation sites for corrosion. Most often, the Mg_2Si phase dissolves, leaving behind a cavity that acts as a nucleation site for pitting.[14–16,20,21] These observations were made

during investigations carried out on commercial aluminum alloys with low Si/Mg mole ratios.[7,22]

Crevice corrosion is a highly localized form of corrosion that occurs by infiltration of water into closely fitted surfaces. The presence of aggressive ions, such as chloride, often creates extensive localized attack.[14] Metals like aluminum that depend on oxide films or passive layers for corrosion resistance are particularly susceptible to crevice corrosion. Attack from this phenomenon can be aggravated when combined with the presence of crystalline defects such as Mg_2Si precipitates. The possibility exists for reducing drastically the alloy susceptibility to corrosion if its microstructure is modified by appropriate heat treatment prior to usage. The research conducted in this study aimed to determine the corrosion rate of an Al alloy in its cast and aged states, as well as to compare the corrosion rate for both states. Aluminum and its alloys have been used in a wide range of industries due to their favorable characteristics such as high strength-to-weight ratio, excellent formability and resistance to corrosion. Aluminum alloys are increasingly utilized in a diverse array of products, including airplane parts, components for the aerospace industry and the shipbuilding sector.[17,18] These industries require materials with high strength-to-weight ratios and superplasticity. Compared to other metals, aluminum alloys offer superior strength while being lightweight. The development of materials with superplasticity aims to enhance their mechanical and forming properties.[18] Various manufacturing techniques have been employed to fabricate and improve these superplastic materials, such as extrusion, rolling, forging, stir casting, as well as more recent methods like friction stir processing.[17] However, the corrosion resistance of these materials is influenced by factors such as alloy composition, processing history, and environmental exposure. Therefore, understanding the corrosion behavior of these materials is crucial for their effective and sustainable use in various applications. The aim of the presented investigation was to analyze the influence of Mg content on the corrosion behavior of Al alloys in order to contribute to reliable prediction of their behavior and to the development of improved corrosion-resistant Al alloy for specific applications.

EXPERIMENTAL

The investigated alloys were obtained by casting and air-cooling in the Foundry Laboratory at the Faculty of Metallurgy and Technology in Podgorica. A 5.5 kW resistance furnace with a working temperature of 1100 °C was used to obtain the alloys. The melting of the alloys was carried out in a graphite crucible placed in the furnace.

High-purity magnesium was used as an alloying element in the alloys, with the Mg content of 2.42, 3.14 and 7.90 mass % in alloys 1,2 and 3, respectively. Copper, zinc, chromium, and manganese were also used as alloying elements in the alloys. The chemical composition of the obtained alloys was analyzed at the Aluminum Combine Podgorica (KAP) using a non-destructive X-ray quantometer method. The selection of the alloying elements was based on previous research, with a focus on the effect of magnesium content on the corrosion charac-

teristics while keeping the content of other alloying elements approximately constant. After casting, all three alloys were subjected to heat treatment, including heating at 515±5 °C for 6 h and quenching in warm water.

Corrosion and electrochemical potentiodynamic investigations were carried out using accelerated testing equipment – the PAR system consisting of a potentiostat/galvanostat model 273, a differential electrometer, a corrosion cell K0047, a saturated calomel electrode (SCE), auxiliary electrodes – cylindrical electrographite, a computer with corrosion software SOFTCORR 352 II, and a printer. All potentials are expressed on SCE scale.

Corrosion testing was performed using the following methods:

– monitoring the change in corrosion potential over time, $E_{corr} = f(\tau)$;

– polarization resistance method, R_p;

– potentiodynamic method.

A NaCl solution with a concentration of 0.51 M was used as the corrosion medium.

The electrochemical behavior was also assessed using potentiostatic electrochemical impedance spectroscopy (PEIS). The measurements were carried out using a three-electrode cell system in a 0.51 M NaCl solution, with platinum wire and SCE serving as the counter and reference electrodes, respectively. Prior to PEIS measurements, the electrolyte was purged with N_2 for 30 min. A potentiostat/galvanostat SP-240 (BioLogic SAS, Grenoble, France) was used for PEIS measurements at open circuit potential.

Optical images were taken with Leica 20 MP Ultra Wide Angle Lens, f/2.2 aperture camera.

RESULTS AND DISCUSSION

The results of the chemical composition of the obtained alloys are presented in Table I. The table shows the percentage of each alloying element used in the production of the alloys, which is an important factor that can affect their properties, including their resistance to corrosion.

TABLE 1. Results of the chemical composition of Al alloys in mass %

Alloy	Fe	Si	Ti	Cu	Zn	V	Cr	Mn	Mg	Sn	Ni	Pb
L1	0.29	0.12	0.14	0.34	0.59	0.012	0.21	0.33	2.42	0.001	0.002	0.007
L2	0.30	0.12	0.13	0.35	0.62	0.012	0.25	0.25	3.14	0.001	0.002	0.008
L3	0.24	0.14	0.13	0.52	0.83	0.013	0.26	0.29	7.90	0.001	0.002	0.001

Table I shows that these are multi-component alloys with different contents of alloying elements. The table lists the mass percentage of each element in the alloys. It can be observed that the alloys have varying amounts of Mg, Cu, Zn, Cr, Mn and Fe. The presence and the amount of each element in the alloys can significantly affect their properties, such as strength, hardness and corrosion resistance. Therefore, understanding the chemical composition of the alloys is crucial for predicting and controlling their behavior in different applications.

Fig. 1 shows the corrosion potential over time of as-cast Al alloys in 0.51 M NaCl solution. Before starting the polarization measurements, the system needs to be stabilized, which is judged by acceptable stability in time of the corrosion potential. Corrosion potential is monitored upon sample immersion into the electrolyte. From the results shown in Fig. 1, a shift in potential of the tested samples

towards more positive values can be observed. The shift in potential of the alloys towards more positive values is interpreted as passivation, or the formation of an oxide film on the surface of the tested samples. The protective layer becomes thicker and more compact over time. This film prevents the passage of aggressive chloride ions from the solution, thus protecting the material from further corrosion.

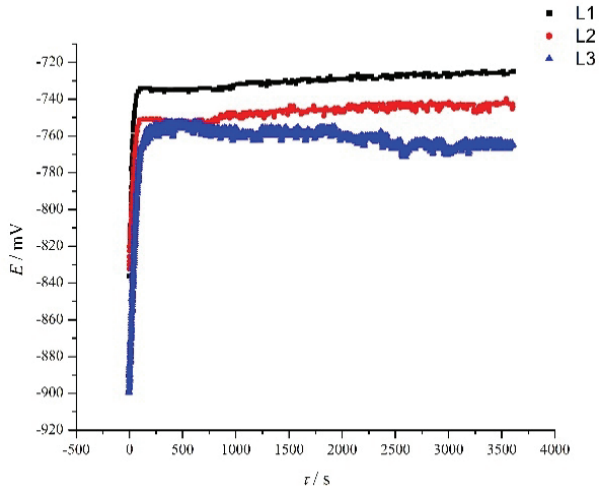

Fig 1. Corrosion potential of as-cast Al alloys over time in 0.51 M NaCl solution.

It can also be seen that corrosion potential takes more positive values as the Mg content increases. This indicates that greater protective ability of the passive films are reached with lower Mg content.

Linear polarization is an electrochemical technique used for monitoring corrosion. It is based on the determination of the polarization resistance, R_p from the slope of the polarization line near the corrosion potential. Based on the results shown in Fig. 2a, and numerical values of the experimental measurements which are shown in Table II, it can be concluded that the samples are stable in the tested solution. Comparing the results, based on the value of the polarization resistance R_p (Table II), it can be observed that there is highest corrosion resistance for the L2 sample, followed by L1 and L3.

Fig. 2b shows the potentiodynamic cathodic and anodic polarization curves of the tested samples in a 0.51 M NaCl solution. In the cathodic region, a small change in current density with potential is observed, indicating a low corrosion rate of the tested samples in the NaCl solution, while in the anodic region, a larger change in current density with potential is observed. The results of the measurements are presented in Table III. Based on the values of j_{corr} and $E_{j=0}$ given in Table III, it can be concluded that L1 is the lowest rate of corrosion in the tested environment, followed by L3 and L2. The potentiodynamic polariz-

ation curves provide valuable information about the corrosion behavior of the materials, as well as the values of the corrosion potential and the current density at which corrosion rate is negligible.

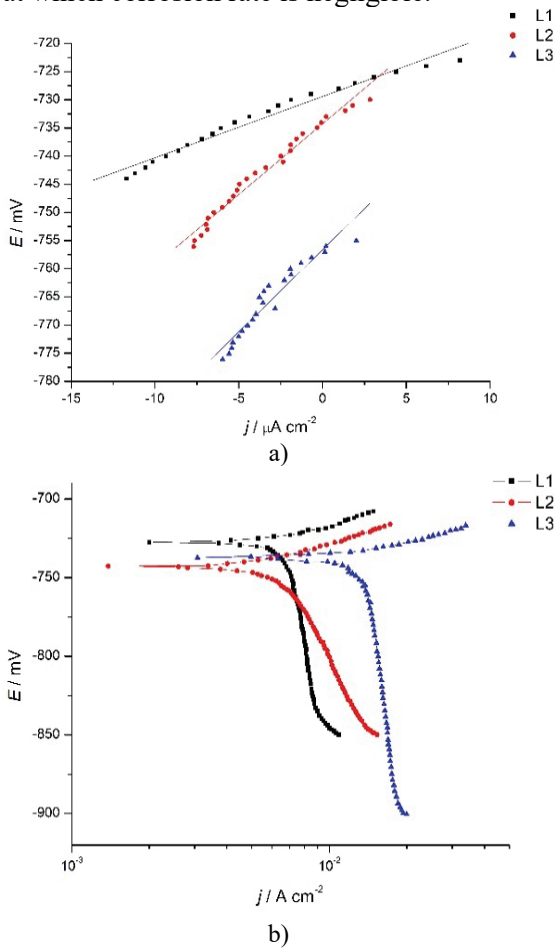

Fig. 2. a) Linear polarization and b) potentiodynamic cathodic and anodic polarization curves of Al alloys in the as-cast state in a 0.51 M NaCl solution.

TABLE II. Change of corrosion potential over time of as-cast Al alloys in a 0.51 M NaCl solution

Sample	E_{start} / mV	E_{fin} / mV
L1	–836	–725
L2	–834	–743
L3	–879	–740

Tables II and III present the complete results of corrosion studies in 0.51 M NaCl on alloys L1, L2 and L3 in as-cast state. The tables provide information on corrosion potential, corrosion current density, polarization resistance, corrosion rate and other related parameters. By analyzing these data, one can gain insight

into the effectiveness of different alloy composition in preventing corrosion and choose the optimal material for specific applications.

TABLE III. Corrosion potential change over time of as-cast Al alloys in a 0.51 M NaCl solution

Sample	$E_{j=0}$ / mV	R_p / kΩ cm^{-2}	β_a / mV	j_{corr} / μA cm^{-2}
L1	–727.5	1.106	19.63	19.64
L2	–743.3	2.554	25.57	8.503
L3	–736.7	0.4605	16.93	47.15

Fig. 3 shows the impedance characteristics of the cast samples upon initial (24 h) and prolonged (120 h) exposure to chloride-containing corrosive medium as impedance complex plane plots.

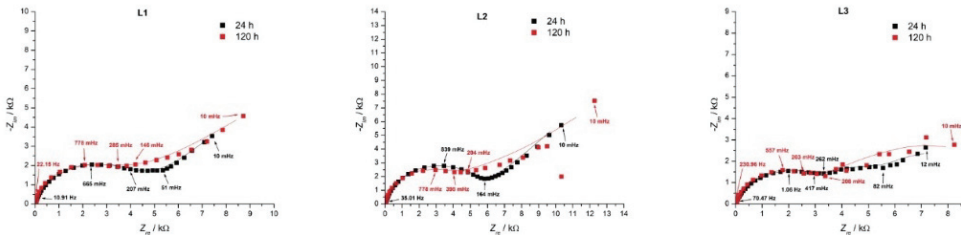

Fig. 3. Impedance complex plane plots of as-cast Al–Mg alloy samples upon initial (24 h) and prolonged (120 h) exposure to 0.51 M NaCl solution. Symbols: registered data; lines: the data of equivalent electrical circuit.

Complex plane spectra of all samples feature high-frequency loop, which is, in the cases of lower Mg content (L1 and L2), followed by well-defined semi-infinite diffusion impedance characteristics at low frequencies. Prolonged exposure causes the deviation of a near-45°-inclined straight line to more resistance-defined behavior as the corrosion proceeds. This indicates the transition from semi-infinite to more noticeable finite diffusion conditions due to the generation and growth of a passive layer on the sample surface. While electrolyte species participating in the corrosion processes diffuse initially from the electrolyte bulk, the corrosion-induced formation of defined porous structure of a layer makes dominant the finite diffusion through the pores upon prolonged exposure. The layer over L3 sample of highest Mg content seems to be formed much quickly, since finite diffusion characteristics are more resolved already in the initial stage of exposure. The photographs of corroded samples (Fig. 4) show that the surface layer of L3 appears the most compact with the least frequent pitting corrosion sites. However, the radii of corrosion products (white zones) around pits are largest, which indicates that pitting corrosion is dominant mechanism in the initial stage. According to Fig. 4, it appears that the increase in Mg content favors the pitting corrosion and induces the formation of more compact passive layer. The

most compact layer apparently causes the most pronounced and well-resolved finite diffusion features in the impedance spectra of L3. The differences between the properties of a layer on L3 and that on L1 and L2 are indicated also by the measures of the high-frequency loop. Although the associated resistances are similar for all of the three samples, the imaginary impedance is lower for L3 due to larger capacitance of a thinner and more compact layer.

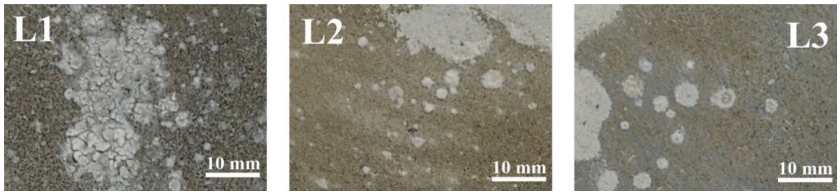

Fig. 4. Optical images of the tested samples after 120 h exposure to 0.51 M NaCl solution.

The considerations of the features of impedance spectra are proved further by the structure of the most suitable equivalent electrical circuit which describes best the physicochemical properties of the samples while they corrode (Fig. 5). The samples of lower Mg content and of less compact passive layers behaves equivalently to the circuit consisted of a parallel connection of capacitor and resistor, which is in series to Randles–Sevcik (R–S) conformation.

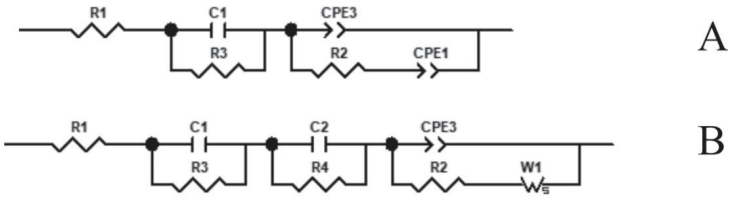

Fig. 5. Equivalent electrical circuits of as-cast Al–Mg alloy samples: a) for L1 and L2 and b) L3 upon initial (24 h) and prolonged (120 h) exposure to 0.51 M NaCl solution.

RC in parallel describes the properties of a layer, whereas R–S relates to diffusion-controlled corrosion processes. Owing to the most distinguishable pitting corrosion and an indication of more compact layer structure, the circuit for L3 required additional RC time constant in series, which indicates the difference between the properties of a bulky layer and that formed around the pits. The values of the circuit parameters are presented in Fig. 6.

The highest values of layer resistance is found for L2 of mid Mg content, associated to the lowest layer capacitance, which indicates the thickest layer is formed on this sample. In Fig. 4 it can be seen that massive layer is formed over the sample surface except the areas close to the sample surface, where pitting corrosion appears dominant. The formation of a massive layer is followed by

considerable increase in charge transfer resistance (R2, which was the lowest initially) and double layer capacitance (CPE-T3). This indicates that corrosion processes take place much faster on L2 than on L1 and L3; however, fast corrosion produces the thickest layer, whose porous structure did not change significantly while the layer grows (initial layer resistance and diffusion admittance are similar to those found upon prolonged exposure (day 1–day 5). Consequently, the corrosion proceeds at the sample surface accessible through the pores of the layers, which area is considerably smaller with respect to L1 and L3. Hence the R2 and CPE-T3 for L2 are considerably larger.

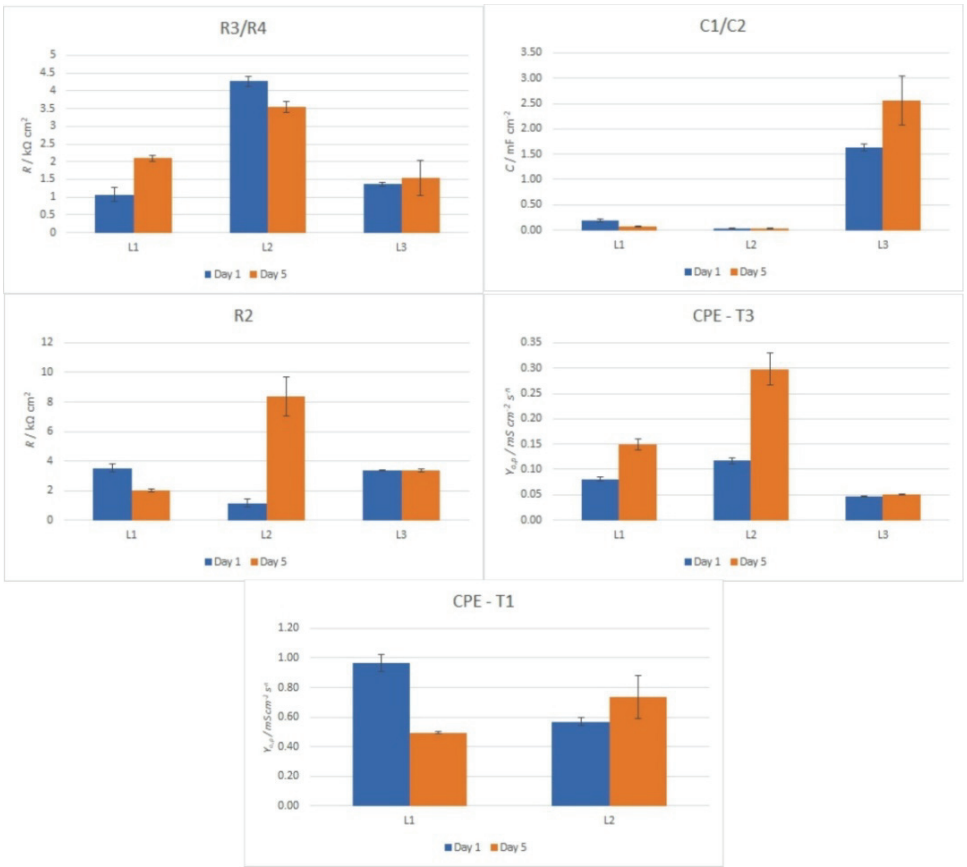

Fig. 6. The values of circuit parameters of the investigated samples; R3/R4 and C1/C2 – resistances and capacitances of the passive layer; R2 and CPE-T3 – charge transfer and double layer capacitance (the values of CPE exponent are above 0.75) associated to corrosion processes; CPE-T1 – diffusion admittance.

Layer resistance of L1 considerably increases during exposure, but it is still lower than the resistance found for L2. This increase is associated with the lowest

charge transfer resistance and diffusion admittance among the samples upon prolonged exposure. This finding is the strong indication of the highly porous layer, unable to slow down the corrosion rate at the layer/sample surface interface. Huge pores homogeneously distributed over the layer surface are also seen in Fig. 4, and even appearance of a cracks around the pits in the middle of the sample is clearly visible. It can be concluded that the L1–L2 increase in Mg content improves the corrosion resistance and clearly separates bulky corrosion from localized pitting corrosion. However, it increases the thickness of more compact, poorly adhesive, layer.

Further increase in Mg content applied in L3 decreases additionally the layer thickness and makes it considerably more compact, which should be beneficial for the formation of a more adherent protective film. This is reflected in the highest layer capacitance and diffusion admittance that is for L3 straightforwardly defined by finite diffusion mechanism (finite Warburg element was only suitable in equivalent circuit for L3, whereas classical Warburg element met the requirement to describe the diffusion in the cases of L1 and L3). However, for the applied exposure the growth rate of a layer was apparently not adequate for the remarkable closing of the pits, since the increase in charge transfer resistance and double layer capacitance was not registered for L3 upon prolonged exposure. The weakness of L3 sample toward the pit activity could be connect to the presence of additional RC time constant, of quite different values of the parameters with respect to that for a layer. Namely, the resistance is much lower, few tens of Ω, and even deceases to *ca*. 8 Ω upon prolonged exposure. The associated capacitance is close to 0.1 mF, which is much lower than that of a layer – thus indicating its highly localized appearance on the surface. Despite this poor immunity of L3 sample toward pitting corrosion, the registered propagation of the properties of a protective layer during 5-day exposure should be expected to show protective features upon much longer exposures to corrosive medium.

CONCLUSION

The article describes the results of an experiment aimed at investigating the corrosion behavior of as-cast Al alloys in NaCl solution. The study employed different electrochemical techniques, including corrosion potential measurements, linear polarization and potentiodynamic polarization curves, as well as impedance measurements. The results show that the Al alloys form a protective oxide film on the surface, which prevents the passage of aggressive chloride ions from the solution, thus protecting the material from further corrosion.

The study found that the impedance characteristics of the cast samples change upon initial and prolonged exposure to the chloride-containing corrosive medium. The complex plane spectra of all samples feature a high-frequency loop followed by well-defined semi-infinite diffusion impedance characteristics at low

frequencies. Prolonged exposure causes the deviation of a near-45°-inclined straight line to more resistance-defined behavior as the corrosion proceeds. The most compact layer apparently causes the most pronounced and well-resolved finite diffusion features in the impedance spectra of L3. The article concludes that the increase in Mg content favors the pitting corrosion and induces the formation of a more compact passive layer.

The study used the most suitable equivalent electrical circuit to describe the physicochemical properties of the samples while they corrode. The samples of lower Mg content and less compact passive layers behave equivalently to the circuit consisted of a parallel connection of a capacitor and resistor, which is in series to the Randles–Sevcik conformation. The circuit for L3 required an additional RC time constant in series, indicating the difference between the properties of a bulky layer and that formed around the pits. The highest values of the layer resistance are found for L2 of mid Mg content, associated with thicker and more compact layers. These results provide insights into the corrosion behavior of as-cast Al alloys and can be useful for the design of new alloys with better corrosion resistance.

In conclusion, the study investigated the corrosion behavior of as-cast Al alloys in NaCl solution, using various electrochemical techniques. The study found that the Al alloys form a protective oxide film on the surface, which prevents the passage of aggressive chloride ions from the solution, thus protecting the material from further corrosion. The study also found that the impedance characteristics of the cast samples change upon initial and prolonged exposure to the chloride-containing corrosive medium, and that the increase in Mg content favors the pitting corrosion and induces the formation of a more compact passive layer. These results provide insights into the corrosion behavior of as-cast Al alloys and can be useful for the design of new alloys with better corrosion resistance. The findings of this study can have significant implications for the development of new corrosion-resistant alloys for a variety of applications. The results demonstrate that the corrosion behavior of Al alloys can be controlled by the composition of the alloy and the formation of a protective oxide layer on the surface. Overall, the study highlights the importance of understanding the corrosion behavior of materials and provides a valuable contribution.

Acknowledgement. This work was supported by the Ministry of Science, Technological Development and Innovation of the Republic of Serbia, Grant No. 451-03-47/2023-01/ /200026.

ИЗВОД

ИМПЕДАНСНИ ОДЗИВ АЛУМИНИЈУМСКИХ ЛЕГУРА СА РАЗЛИЧИТИМ САДРЖАЈЕМ МАГНЕЗИЈУМА ТОКОМ ИЗЛОЖЕНОСТИ ХЛОРИДНОЈ КОРОЗИОНОЈ СРЕДИНИ

ЈЕЛЕНА ШЋЕПАНОВИЋ[1], МАРИЈАНА Р. ПАНТОВИЋ ПАВЛОВИЋ[2,3], ДАРКО ВУКСАНОВИЋ[1], ГАВРИЛО М. ШЕКУЛАРАЦ[2] и МИРОСЛАВ М. ПАВЛОВИЋ[2,3]

[1]Металуршко-технолошки факултет, Универзитет у Црној Гори, Подгорица, Црна Гора, [2]Институт за хемију, технологију и металургију, Институт од националног значаја за Републику Србију, Центар за електрохемију, Универзитет у Београду, Београд и [3]Центар изузетних вредности за хемију и инжењеринг животне средине, Институт за хемију, технологију и металургију, Београд

Ово истраживање се бави понашањем корозије Al легура са различитим садржајем Mg уз примену потенциостатске електрохемијске импедансне спектроскопије (PEIS). Спектри у комплексној равни свих узорака се карактеришу петљом високе фреквенције праћеном карактеристикама полу-бесконачне дифузије на ниским фреквенцијама, са формирањем дефинисане порозне структуре слоја услед корозије, што доводи до доминације коначне дифузије кроз поре при продуженој изложености. Најкомпактнији слој узрокује најизраженије и најјасније карактеристике коначне дифузије у импедансним спектрима узорка са највећим садржајем Mg, док узорак са најмањим садржајем Mg има високо порозан слој који не може успорити брзину корозије на граници фаза слој/узорак. Највећу капацитивност и адмитанцију дифузионог слоја има узорак са највећим садржајем Mg, са очекиваном појавом адекватног заштитног филма. Међутим, брзина раста слоја није била довољна за значајно затварање питова, што указује на слабост овог узорка према питинг корозији. Резултати показују да повећање садржаја Mg побољшава отпорност на корозију и јасно раздваја корозију у маси материјала од локализоване питинг корозије, али истовремено повећава дебљину слоја који је слабије адхезије и компактнији.

(Примљено 5. маја, ревидирано 23. јуна, прихваћено 1. јула 2023)

REFERENCES

1. X. Zhang, M. Zhang, R. Li, X. Feng, X. Pang, J. Rao, D. Cong, C. Yin, Y. Zhang, *Coatings* **11** (2021) (https://doi.org/10.3390/coatings11111316)
2. K. A. Yasakau, M. L. Zheludkevich, S. V Lamaka, M. G. S. Ferreira, *Electrochim. Acta* **52** (2007) 7651 (https://doi.org/10.1016/j.electacta.2006.12.072)
3. L. Garrigues, N. Pebere, F. Dabosi, *Electrochim. Acta* **41** (1996) 1209 (https://doi.org/10.1016/0013-4686(95)00472-6)
4. S. O. Adeosun, O. I. Sekunowo, S. A. Balogun, V. D. Obiekea, *Int. J. Corros.* **2012** (2012) 927380 (https://doi.org/10.1155/2012/927380)
5. S. P. B., T. U. Dhanaji, S. Dassani, M. Somasundaram, A. Muthuchamy, A. Raja Annamalai, *Crystals* **13** (2023) (https://doi.org/10.3390/cryst13020344)
6. B. Li, Z. Zhang, T. Liu, Z. Qiu, Y. Su, J. Zhang, C. Lin, L. Wang, *Materials (Basel, Switzerland)* **15** (2022) (https://doi.org/10.3390/ma15113912)
7. S. Ren, X. He, X. Qu, I. S. Humail, Y. Li, *Mater. Sci. Eng., B* **138** (2007) 263 (https://doi.org/10.1016/j.mseb.2007.01.023)
8. F. Andreatta, H. Terryn, J. H. W. de Wit, *Corros. Sci.* **45** (2003) 1733 (https://doi.org/10.1016/S0010-938X(03)00004-0)
9. M. Popović, E. Romhanji, *Mater. Sci. Eng., A* **492** (2008) 460 (https://doi.org/10.1016/j.msea.2008.04.001)

10. L. Ren, H. Gu, W. Wang, S. Wang, C. Li, Z. Wang, Y. Zhai, P. Ma, *Materials (Basel, Switzerland)* **12** (2019) (https://doi.org/10.3390/ma12244160)
11. H. P. Godard, *The corrosion of light metals*, Wiley, New York, 1967, ISBN: 978-0471308614
12. A. D. Cristian, M. M. Georgiana, S. A. Victor, M. M. A. B. Abdullah, *AIP Conf. Proc.* **1835** (2017) 20051 (https://doi.org/10.1063/1.4983791)
13. N. Loukil, in *Magnesium Alloys Structure and Properties*, T. Tański, P. Jarka, Eds., IntechOpen, Rijeka, 2021, p. 833 (https://doi.org/10.5772/intechopen.96232)
14. S. K. Kairy, P. A. Rometsch, K. Diao, J. F. Nie, C. H. J. Davies, N. Birbilis, *Electrochim. Acta* **190** (2016) 92 (https://doi.org/10.1016/j.electacta.2015.12.098)
15. F. Song, X. Zhang, S. Liu, Q. Tan, D. Li, *Corros. Sci.* **78** (2014) 276 (https://doi.org/10.1016/j.corsci.2013.10.010)
16. C. Brito, T. Vida, E. Freitas, N. Cheung, J. E. Spinelli, A. Garcia, *J. Alloys Compd.* **673** (2016) 220 (https://doi.org/10.1016/j.jallcom.2016.02.161)
17. M. M. Tawfik, M. M. Nemat-Alla, M. M. Dewidar, *J. Mater. Res. Technol.* **13** (2021) 754 (https://doi.org/https://doi.org/10.1016/j.jmrt.2021.04.076)
18. J. Liu, M.-J. Tan, A.-E.-W. Jarfors, Y. Aue-u-lan, S. Castagne, *Mater. Des.* **31** (2010) S66 (https://doi.org/10.1016/j.matdes.2009.10.052)
19. J. H. W. de Wit, *Electrochim. Acta* **49** (2004) 2841 (https://doi.org/10.1016/j.electacta.2004.01.045)
20. N. Birbilis, R. G. Buchheit, *J. Electrochem. Soc.* **152** (2005) B140 (https://doi.org/10.1149/1.1869984)
21. J. Wloka, G. Bürklin, S. Virtanen, *Electrochim. Acta* **53** (2007) 2055 (https://doi.org/10.1016/j.electacta.2007.09.004)
22. A. Pardo, M. C. Merino, R. Arrabal, S. Merino, F. Viejo, A. E. Coy, *Appl. Surf. Sci.* **252** (2006) 2794 (https://doi.org/10.1016/j.apsusc.2005.04.023).